1-1999

Search for invisible Higgs boson decays in e+e- collisions at centre-of-mass energies up to 184 GeV

R. BARATE

Manoj THULASIDAS
Singapore Management University, manojt@smu.edu.sg

EUROPEAN LABORATORY FOR PARTICLE PHYSICS (CERN)

CERN-EP/99-008
21 January 1999

Search for invisible Higgs boson decays in e^+e^- collisions at centre-of-mass energies up to 184 GeV

The ALEPH Collaboration *)

Abstract

In a data sample of 78.3 pb^{-1} collected in 1996 and 1997 by the ALEPH detector at centre-of-mass energies from 161 to 184 GeV, invisible decays of a Higgs boson have been searched for in the reaction $e^+e^- \to hZ$, where the Z can decay into e^+e^-, $\mu^+\mu^-$ or $q\bar{q}$. No evidence for a signal is found and limits on the production cross section are derived as a function of the Higgs boson mass. These results are combined with those obtained in an update of the analyses of the ALEPH data taken at LEP 1. For a production cross section equal to that of the minimal standard model Higgs boson, masses below 80 GeV/c^2 are excluded at 95% C.L.

(Submitted to Physics Letters)

*) See next pages for the list of authors

The ALEPH Collaboration

R. Barate, D. Decamp, P. Ghez, C. Goy, S. Jezequel, J.-P. Lees, F. Martin, E. Merle, M.-N. Minard, J.-Y. Nief, B. Pietrzyk

Laboratoire de Physique des Particules (LAPP), IN^{2}P^3-CNRS, F-74019 Annecy-le-Vieux Cedex, France

R. Alemany, M.P. Casado, M. Chmeissani, J.M. Crespo, M. Delfino, E. Fernandez, M. Fernandez-Bosman, Ll. Garrido,[15] E. Graugès, A. Juste, M. Martinez, G. Merino, R. Miquel, Ll.M. Mir, P. Morawitz, A. Pacheco, I.C. Park, A. Pascual, I. Riu, F. Sanchez

Institut de Física d'Altes Energies, Universitat Autònoma de Barcelona, 08193 Bellaterra (Barcelona), E-Spain[7]

A. Colaleo, D. Creanza, M. de Palma, G. Gelao, G. Iaselli, G. Maggi, M. Maggi, S. Nuzzo, A. Ranieri, G. Raso, F. Ruggieri, G. Selvaggi, L. Silvestris, P. Tempesta, A. Tricomi,[3] G. Zito

Dipartimento di Fisica, INFN Sezione di Bari, I-70126 Bari, Italy

X. Huang, J. Lin, Q. Ouyang, T. Wang, Y. Xie, R. Xu, S. Xue, J. Zhang, L. Zhang, W. Zhao

Institute of High-Energy Physics, Academia Sinica, Beijing, The People's Republic of China[8]

D. Abbaneo, U. Becker,[22] G. Boix,[2] M. Cattaneo, V. Ciulli, G. Dissertori, H. Drevermann, R.W. Forty, M. Frank, F. Gianotti, A.W. Halley, J.B. Hansen, J. Harvey, P. Janot, B. Jost, I. Lehraus, O. Leroy, C. Loomis, P. Maley, P. Mato, A. Minten, A. Moutoussi, F. Ranjard, L. Rolandi, D. Rousseau, D. Schlatter, M. Schmitt,[12] O. Schneider,[23] W. Tejessy, F. Teubert, I.R. Tomalin, E. Tournefier, M. Vreeswijk, A.E. Wright

European Laboratory for Particle Physics (CERN), CH-1211 Geneva 23, Switzerland

Z. Ajaltouni, F. Badaud G. Chazelle, O. Deschamps, S. Dessagne, A. Falvard, C. Ferdi, P. Gay, C. Guicheney, P. Henrard, J. Jousset, B. Michel, S. Monteil, J-C. Montret, D. Pallin, P. Perret, F. Podlyski

Laboratoire de Physique Corpusculaire, Université Blaise Pascal, IN^{2}P^3-CNRS, Clermont-Ferrand, F-63177 Aubière, France

J.D. Hansen, J.R. Hansen, P.H. Hansen, B.S. Nilsson, B. Rensch, A. Wäänänen

Niels Bohr Institute, 2100 Copenhagen, DK-Denmark[9]

G. Daskalakis, A. Kyriakis, C. Markou, E. Simopoulou, A. Vayaki

Nuclear Research Center Demokritos (NRCD), GR-15310 Attiki, Greece

A. Blondel, J.-C. Brient, F. Machefert, A. Rougé, M. Swynghedauw, R. Tanaka, A. Valassi,[6] H. Videau

Laboratoire de Physique Nucléaire et des Hautes Energies, Ecole Polytechnique, IN^{2}P^3-CNRS, F-91128 Palaiseau Cedex, France

E. Focardi, G. Parrini, K. Zachariadou

Dipartimento di Fisica, Università di Firenze, INFN Sezione di Firenze, I-50125 Firenze, Italy

R. Cavanaugh, M. Corden, C. Georgiopoulos

Supercomputer Computations Research Institute, Florida State University, Tallahassee, FL 32306-4052, USA [13,14]

A. Antonelli, G. Bencivenni, G. Bologna,[4] F. Bossi, P. Campana, G. Capon, F. Cerutti, V. Chiarella, P. Laurelli, G. Mannocchi,[5] F. Murtas, G.P. Murtas, L. Passalacqua, M. Pepe-Altarelli[1]

Laboratori Nazionali dell'INFN (LNF-INFN), I-00044 Frascati, Italy

M. Chalmers, L. Curtis, J.G. Lynch, P. Negus, V. O'Shea, B. Raeven, C. Raine, D. Smith, P. Teixeira-Dias, A.S. Thompson, J.J. Ward

Department of Physics and Astronomy, University of Glasgow, Glasgow G12 8QQ,United Kingdom[10]

O. Buchmüller, S. Dhamotharan, C. Geweniger, P. Hanke, G. Hansper, V. Hepp, E.E. Kluge, A. Putzer, J. Sommer, K. Tittel, S. Werner,[22] M. Wunsch

Institut für Hochenergiephysik, Universität Heidelberg, D-69120 Heidelberg, Germany[16]

R. Beuselinck, D.M. Binnie, W. Cameron, P.J. Dornan,[1] M. Girone, S. Goodsir, N. Marinelli, E.B. Martin, J. Nash, J. Nowell, J.K. Sedgbeer, P. Spagnolo, E. Thomson, M.D. Williams

Department of Physics, Imperial College, London SW7 2BZ, United Kingdom[10]

V.M. Ghete, P. Girtler, E. Kneringer, D. Kuhn, G. Rudolph

Institut für Experimentalphysik, Universität Innsbruck, A-6020 Innsbruck, Austria[18]

A.P. Betteridge, C.K. Bowdery, P.G. Buck, P. Colrain, G. Crawford, G. Ellis, A.J. Finch, F. Foster, G. Hughes, R.W.L. Jones, N.A. Robertson, M.I. Williams

Department of Physics, University of Lancaster, Lancaster LA1 4YB, United Kingdom[10]

P. van Gemmeren, I. Giehl, F. Hölldorfer, C. Hoffmann, K. Jakobs, K. Kleinknecht, M. Kröcker, H.-A. Nürnberger, G. Quast, B. Renk, E. Rohne, H.-G. Sander, S. Schmeling, H. Wachsmuth C. Zeitnitz, T. Ziegler

Institut für Physik, Universität Mainz, D-55099 Mainz, Germany[16]

J.J. Aubert, C. Benchouk, A. Bonissent, J. Carr,[1] P. Coyle, A. Ealet, D. Fouchez, F. Motsch, P. Payre, M. Talby, M. Thulasidas, A. Tilquin

Centre de Physique des Particules, Faculté des Sciences de Luminy, IN^{2}P^3-CNRS, F-13288 Marseille, France

M. Aleppo, M. Antonelli, F. Ragusa

Dipartimento di Fisica, Università di Milano e INFN Sezione di Milano, I-20133 Milano, Italy.

R. Berlich, V. Büscher, H. Dietl, G. Ganis, K. Hüttmann, G. Lütjens, C. Mannert, W. Männer, H.-G. Moser, S. Schael, R. Settles, H. Seywerd, H. Stenzel, W. Wiedenmann, G. Wolf

Max-Planck-Institut für Physik, Werner-Heisenberg-Institut, D-80805 München, Germany[16]

P. Azzurri, J. Boucrot, O. Callot, S. Chen, M. Davier, L. Duflot, J.-F. Grivaz, Ph. Heusse, A. Jacholkowska, M. Kado, J. Lefrançois, L. Serin, J.-J. Veillet, I. Videau,[1] J.-B. de Vivie de Régie, D. Zerwas

Laboratoire de l'Accélérateur Linéaire, Université de Paris-Sud, IN^{2}P^3-CNRS, F-91898 Orsay Cedex, France

G. Bagliesi, S. Bettarini, T. Boccali, C. Bozzi, G. Calderini, R. Dell'Orso, I. Ferrante, A. Giassi, A. Gregorio, F. Ligabue, A. Lusiani, P.S. Marrocchesi, A. Messineo, F. Palla, G. Rizzo, G. Sanguinetti, A. Sciabà, G. Sguazzoni, R. Tenchini, C. Vannini, A. Venturi, P.G. Verdini

Dipartimento di Fisica dell'Università, INFN Sezione di Pisa, e Scuola Normale Superiore, I-56010 Pisa, Italy

G.A. Blair, J. Coles, G. Cowan, M.G. Green, D.E. Hutchcroft, L.T. Jones, T. Medcalf, J.A. Strong, J.H. von Wimmersperg-Toeller

Department of Physics, Royal Holloway & Bedford New College, University of London, Surrey TW20 OEX, United Kingdom[10]

D.R. Botterill, R.W. Clifft, T.R. Edgecock, P.R. Norton, J.C. Thompson

Particle Physics Dept., Rutherford Appleton Laboratory, Chilton, Didcot, Oxon OX11 OQX, United Kingdom[10]

B. Bloch-Devaux, P. Colas, B. Fabbro, G. Faïf, E. Lançon, M.-C. Lemaire, E. Locci, P. Perez, H. Przysiezniak, J. Rander, J.-F. Renardy, A. Rosowsky, A. Trabelsi,[20] B. Tuchming, B. Vallage

CEA, DAPNIA/Service de Physique des Particules, CE-Saclay, F-91191 Gif-sur-Yvette Cedex, France[17]

S.N. Black, J.H. Dann, H.Y. Kim, N. Konstantinidis, A.M. Litke, M.A. McNeil, G. Taylor

Institute for Particle Physics, University of California at Santa Cruz, Santa Cruz, CA 95064, USA[19]

C.N. Booth, S. Cartwright, F. Combley, P.N. Hodgson, M.S. Kelly, M. Lehto, L.F. Thompson
Department of Physics, University of Sheffield, Sheffield S3 7RH, United Kingdom[10]

K. Affholderbach, A. Böhrer, S. Brandt, C. Grupen, A. Misiejuk, G. Prange, U. Sieler
Fachbereich Physik, Universität Siegen, D-57068 Siegen, Germany[16]

G. Giannini, B. Gobbo
Dipartimento di Fisica, Università di Trieste e INFN Sezione di Trieste, I-34127 Trieste, Italy

J. Putz, J. Rothberg, S. Wasserbaech, R.W. Williams
Experimental Elementary Particle Physics, University of Washington, WA 98195 Seattle, U.S.A.

S.R. Armstrong, E. Charles, P. Elmer, D.P.S. Ferguson, Y. Gao, S. González, T.C. Greening, O.J. Hayes, H. Hu, S. Jin, P.A. McNamara III, J.M. Nachtman,[21] J. Nielsen, W. Orejudos, Y.B. Pan, Y. Saadi, I.J. Scott, J. Walsh, Sau Lan Wu, X. Wu, G. Zobernig
Department of Physics, University of Wisconsin, Madison, WI 53706, USA[11]

[1]Also at CERN, 1211 Geneva 23, Switzerland.
[2]Supported by the Commission of the European Communities, contract ERBFMBICT982894.
[3]Also at Dipartimento di Fisica, INFN Sezione di Catania, 95129 Catania, Italy.
[4]Also Istituto di Fisica Generale, Università di Torino, 10125 Torino, Italy.
[5]Also Istituto di Cosmo-Geofisica del C.N.R., Torino, Italy.
[6]Now at LAL, 91898 Orsay, France.
[7]Supported by CICYT, Spain.
[8]Supported by the National Science Foundation of China.
[9]Supported by the Danish Natural Science Research Council.
[10]Supported by the UK Particle Physics and Astronomy Research Council.
[11]Supported by the US Department of Energy, grant DE-FG0295-ER40896.
[12]Now at Harvard University, Cambridge, MA 02138, U.S.A.
[13]Supported by the US Department of Energy, contract DE-FG05-92ER40742.
[14]Supported by the US Department of Energy, contract DE-FC05-85ER250000.
[15]Permanent address: Universitat de Barcelona, 08208 Barcelona, Spain.
[16]Supported by the Bundesministerium für Bildung, Wissenschaft, Forschung und Technologie, Germany.
[17]Supported by the Direction des Sciences de la Matière, C.E.A.
[18]Supported by Fonds zur Förderung der wissenschaftlichen Forschung, Austria.
[19]Supported by the US Department of Energy, grant DE-FG03-92ER40689.
[20]Now at Département de Physique, Faculté des Sciences de Tunis, 1060 Le Belvédère, Tunisia.
[21]Now at University of California at Los Angeles (UCLA), Los Angeles, CA 90024, U.S.A.
[22]Now at SAP AG, 69185 Walldorf, Germany
[23]Now at Université de Lausanne, 1015 Lausanne, Switzerland.

1 Introduction

Higgs boson decays into invisible final states are predicted by many extensions of the standard model [1]. In these models, the reaction $e^+e^- \to hZ$ may therefore lead to topologies involving acoplanar lepton pairs, when the Z decays to e^+e^- or $\mu^+\mu^-$, or acoplanar pairs of jets, when the Z decays to $q\bar{q}$. In general, the production cross section of this reaction can be expressed as $\xi^2\sigma_{SM}(e^+e^- \to HZ)$, where ξ^2 represents a model-dependent constant which reduces the cross section with respect to that of the production of the standard model Higgs boson H.

In particular, within the minimal supersymmetric extension of the standard model (MSSM), the lighter CP-even Higgs boson h can decay into a pair of lightest neutralinos $h \to \chi\chi$, when the neutralino χ is light enough. This decay leads to an invisible final state under the hypothesis of R-parity conservation. If the gaugino masses are unified at the GUT scale, the negative result of direct chargino searches essentially excludes the possibility of observing such invisible Higgs boson decays at LEP [2]. If, however, this assumption is relaxed, new regions of the parameter space become accessible, thus opening this possibility.

The searches reported in this letter are based on data collected by ALEPH in 1996 at centre-of-mass energies of 161, 170 and 172 GeV with integrated luminosities of 10.9, 1.1 and 9.5 pb^{-1} respectively, and in 1997 at centre-of-mass energies from 181 to 184 GeV with a total integrated luminosity of 56.8 pb^{-1}. The results are combined with an update of the search for the invisible decay modes of the Higgs boson performed at LEP 1 in the monojet and acoplanar lepton topologies [3] and a reinterpretation of the search for acoplanar jets designed for the $e^+e^- \to (H \to \text{hadrons})\nu\bar{\nu}$ channel [4]. A search for invisible Higgs boson decays at LEP 2 has also been performed by L3 [5].

2 The ALEPH detector

A detailed description of the ALEPH detector and its performance can be found in Refs. [6] and [7]. Only a brief description of the detector components and algorithms relevant to this analysis is given here. The major modification to the apparatus with respect to Ref. [6] consists of a new vertex detector which was installed in October 1995. It is twice as long as the previous one, providing a larger acceptance, and has less material in the active region. The tracking system consists of the new vertex detector, an inner tracking chamber and a large time projection chamber, immersed in a 1.5 T axial magnetic field provided by a superconducting solenoidal coil. The momentum resolution of the tracking system is given by $\sigma(1/p_T) = 6 \times 10^{-4} \oplus 5 \times 10^{-3}/p_T$ (p_T in GeV/c). Hereafter, charged particle tracks reconstructed with at least four hits in the time projection chamber and originating from within a cylinder of length 20 cm and radius 2 cm coaxial with the beam and centred at the nominal collision point are referred to as *good tracks*.

The electromagnetic calorimeter, placed between the time projection chamber and the coil, is a highly segmented sampling calorimeter used to identify electrons and photons and to measure their energy, with a relative resolution of $0.18/\sqrt{E} + 0.009$ (E in GeV). The luminosity calorimeters allow the geometrical acceptance to be covered down to 34 mrad from the beam axis. The hadron calorimeter consists of the return yoke of the magnet,

instrumented with streamer tubes. It provides a measurement of the energy of charged and neutral hadrons, with a relative resolution of $0.85/\sqrt{E}$ (E in GeV) and, together with the external muon chambers, muon identification.

The total visible energy, and therefore also the missing energy, are measured with an energy-flow algorithm [7], combining all the aforementioned measurements. This algorithm also provides a list of charged and neutral reconstructed objects, allowing jets to be reconstructed with an angular resolution of 20 mrad both in azimuthal and polar angles and with an energy resolution of $(0.6\sqrt{E} + 0.6)$ GeV (E in GeV).

3 Event selection

The topologies of interest at LEP 2 consist of a pair of leptons or a pair of jets with mass close to m_{Z} and with large missing energy and mass. The signal topologies were simulated at several Higgs boson masses and centre-of-mass energies with the HZHA generator [8]. Monte Carlo samples describing the standard background processes were used to optimize the selection procedures. Dilepton processes were simulated with KORALZ [9] for $\mu^+\mu^-$ and $\tau^+\tau^-$ and UNIBAB [10] for Bhabha production. The $\gamma\gamma$ interactions were simulated by PHOT02 [11], PYTHIA [12] and PHOJET [13], depending on the specific kinematic configurations and final states. A private generator was used to simulate $\mathrm{Z}\nu\bar{\nu}$ final states [14]. All other relevant processes ($\mathrm{q\bar{q}}\gamma$, $\mathrm{W^+W^-}$, ZZ, $\mathrm{We}\nu$ and $\mathrm{Ze^+e^-}$) were simulated with PYTHIA. As a cross check, the four-fermion processes were also generated using KORALW [15].

The optimizations of the selections for the LEP 1, 1996 and 1997 data samples were performed separately using the method described in Ref. [16] and their combination was done using the elitist prescription described therein. The selection procedures described below were optimized for a Higgs boson mass value of 67 GeV/c^2 at 161 and at 170–172 GeV and for a mass value of 80 GeV/c^2 at 181–184 GeV. The LEP 1 monojet analysis was optimized for a Higgs boson mass of 67 GeV/c^2. No background subtraction was performed in any of the channels analysed.

3.1 The acoplanar lepton pair topology

To select hZ final states where the Z decays leptonically and the Higgs boson invisibly, events are required to have only two good tracks, which must be identified either as an electron pair or a muon pair [7]. Only leptons well contained in the detector are selected by requiring $|\cos\theta_1| + |\cos\theta_2| < 1.85$, where $\theta_{1,2}$ are the polar angles of the leptons with respect to the beam axis. In addition, the acollinearity, defined as the angle between the two lepton directions, is required to be greater than 125°.

To reject the background from $\mathrm{e^+e^-} \to \mathrm{e^+e^-}$ and $\mu^+\mu^-$, the visible energy is required to be less than 65% of the centre-of-mass energy and the acoplanarity, defined as the azimuthal angle between the two lepton directions, must be less than 175°. The background contribution from the $\gamma\gamma \to \ell^+\ell^-$ processes is reduced by requiring the total transverse momentum p_T to be greater than 12.5, 15 and 17 GeV/c, at 161, 170–172 and 181–184 GeV, respectively.

From the measured transverse momenta of the two leptons, $p_{\perp,i}(i = 1, 2)$, and their error estimates, $\sigma_{1/p_{\perp,i}}$, a χ^2 measuring the consistency of the lepton pair mass m with the Z mass and defined as

$$\chi^2 = \sum_{i=1,2} \frac{\left(1/p_{\perp,i} - 1/p^0_{\perp,i}\right)^2}{\sigma^2_{1/p_{\perp,i}}} - 2\log \frac{m^2_{\rm Z}\Gamma^2_{\rm Z}}{(m^2(p^0_{\perp,i}) - m^2_{\rm Z})^2 + m^2_{\rm Z}\Gamma^2_{\rm Z}} \ ,$$

is minimized with respect to $p^0_{\perp,i}$. Events with a χ^2 greater than 5.0 are rejected. The χ^2 distribution is shown in Fig. 1 for data and Monte Carlo at 181–184 GeV, after the requirements of two identified leptons and of p_T greater than 5 GeV/c.

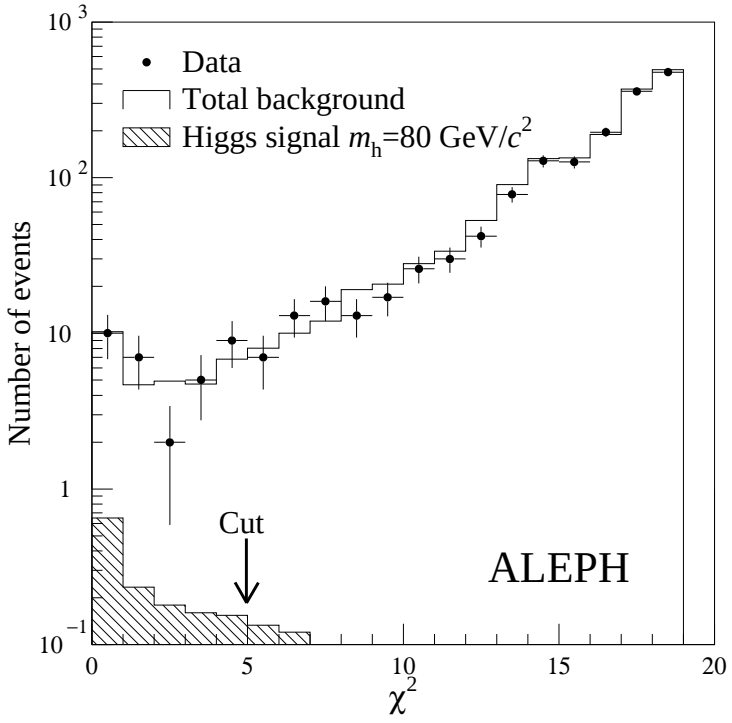

Figure 1: Comparison between the 181–184 GeV data (dots with error bars) and the standard model expectation (open histogram) for the χ^2 distribution of the leptonic sample. The signal expectation for the standard production cross section is represented by the hatched histogram. Some cuts were relaxed to preserve sufficient statistics.

The efficiency of the acoplanar lepton pair selection is shown in Fig. 2a as a function of the Higgs boson mass for the various centre-of-mass energies. The systematic uncertainty on the efficiency was estimated to be 6%, dominated by the Monte Carlo statistics, the lepton identification and the estimate of $\sigma_{1/p_\perp}$.

One candidate event was observed in the 181–184 GeV data sample; its fitted missing mass is 83.2 GeV/c^2, with a resolution of 3 GeV/c^2. No candidate events were observed in the 161 and 170–172 GeV data samples. The expected background comes mainly from four-fermion processes and amounts to 0.1 events for data collected at 161 GeV, to 0.2 events for data collected at 170–172 GeV and to 1.0 event for data collected at 181–184 GeV.

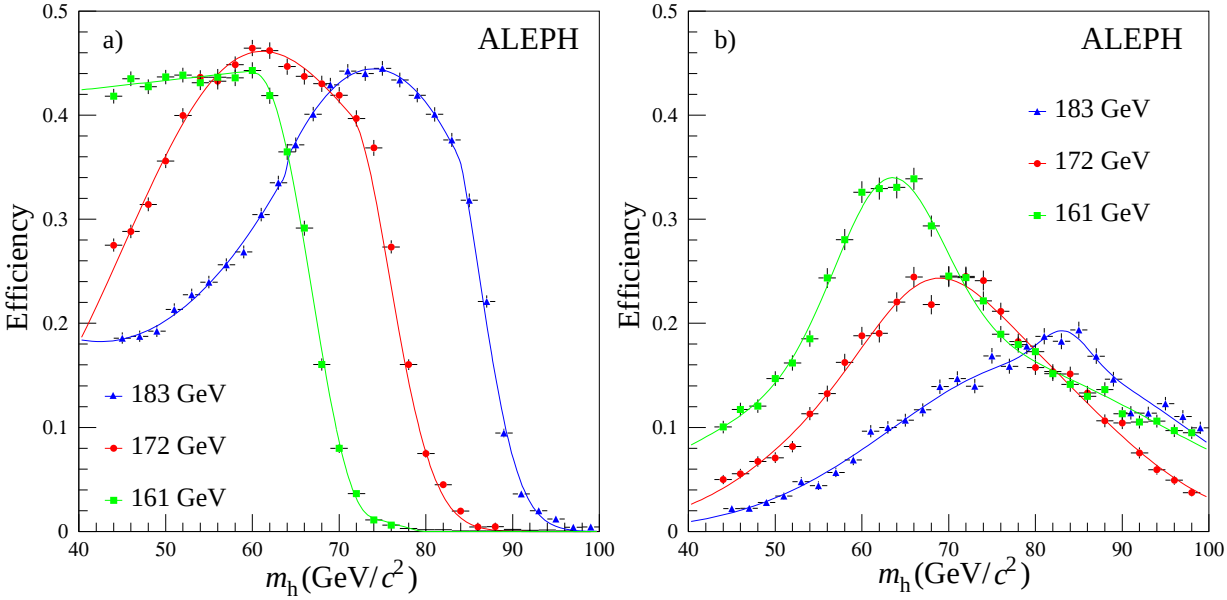

Figure 2: Efficiencies for the (a) acoplanar lepton pair, and (b) acoplanar jet pair analyses at 161, 170–172 GeV and 181–184 GeV. The curves represent the parametrization used to set limits.

3.2 The acoplanar jet pair topology

Events coming from $e^+e^- \to hZ$ with Z decaying into hadrons and h invisibly are selected by requiring at least five good tracks which account for at least 10% of the centre-of-mass energy. The missing momentum must point away from the beam axis ($|\cos\theta_{\rm mis}| < 0.9$) to avoid final states with undetected energetic particles at low polar angles. Background from two-photon collisions is further reduced by requiring that the total transverse momentum be larger than 5 GeV/c.

To suppress the WW background, where one W decays leptonically and the other hadronically, no identified lepton with a momentum greater than 15 GeV/c must be found in the event. In addition, the most isolated good track, defined as the track making the largest angle with its closest track, must not be identified as a lepton and must have a momentum smaller than 5 GeV/c. The distribution of the visible mass is shown in Fig. 3 for the 181–184 GeV data sample. Only events with visible mass between 70 and 100 GeV/c^2 are kept.

The other selection cuts, optimized at the different centre-of-mass energies, are listed in Table 1.

For example, at 181–184 GeV, in order to reduce $e^+e^- \to q\bar{q}$ background events the visible energy is required to be less than 115 GeV. To reject radiative return events, the transverse acoplanarity angle, defined in Ref. [17], must be less than 170°, the acollinearity greater than 120°, and the acoplanarity, defined in Ref. [18], larger than 0.15.

To tackle the Weν and WW backgrounds, a b-tagging neural network [19] is employed. The events are first forced to form two jets using the Durham algorithm, with a threshold value of the jet clustering variable y_{12} for which the event topology changes from one jet to two jets in excess of 0.5. To select hZ events in which the Z decays to $b\bar{b}$, the sum of

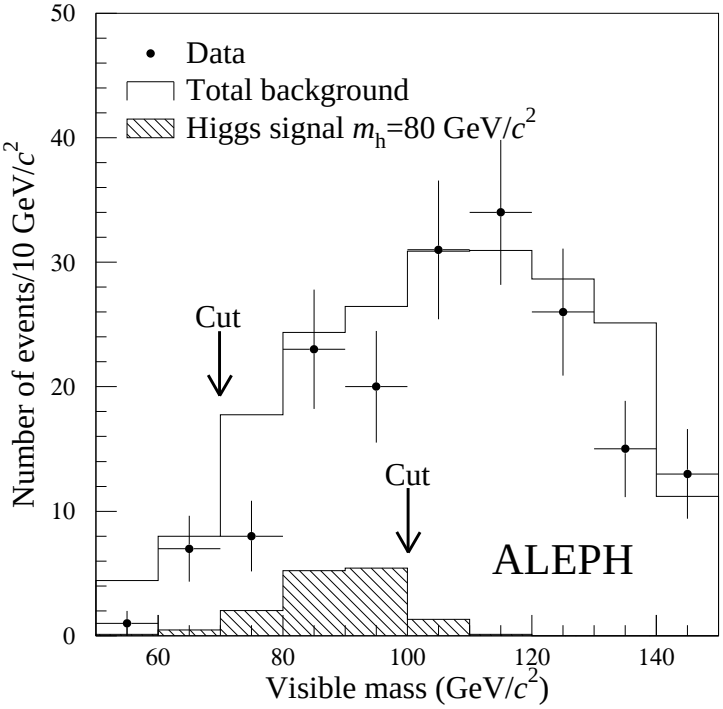

Figure 3: Comparison between the 181–184 GeV data (dots with error bars) and the standard model expectation (open histogram) for the visible mass distribution of the hadronic sample. The signal expectation for the standard production cross section is represented by the hatched histogram. Some cuts were relaxed to preserve sufficient statistics.

the two hemisphere neural network outputs η is required to be greater than 1.5. To select with some efficiency the hZ events where Z does not decay to $b\bar{b}$, events with a smaller η value are kept for which more stringent kinematic cuts must be applied. These events are forced to form three jets, again using the Durham algorithm. The minimum dijet angle is required to be less than 40°, and the smallest dijet invariant mass smaller than 20 GeV/c^2. At 161 GeV, however, there is much less background coming from WW events and the anti-WW cuts are not applied. Instead, to remove the significant contribution of $q\bar{q}(\gamma)$ events, each of the three jets must contain at least one charged particle, and the sphericity must be less than 0.15.

The efficiency of the jet pair selection is shown in Fig. 2b as a function of the Higgs boson mass for the various centre-of-mass energies. The systematic error on the efficiency was estimated to be 5%, dominated by the Monte Carlo statistics and possible inaccuracies in the energy flow simulation.

One candidate event was observed in the 181–184 GeV data sample, with a missing mass of 90.9 GeV/c^2 and a resolution of 7 GeV/c^2; no candidates were observed in the lower energy data. The expected background mainly comes from four-fermion processes and it amounts, according to PYTHIA, to 0.75, 0.84, and 3.46 events at 161, 170–172 and 181–184 GeV, respectively. The deficit of events in the chosen visible mass range (70–100 GeV/c^2) is already present for looser cuts, as shown in Fig. 3 where the Monte Carlo background distribution is based on the PYTHIA generator. The background expectation based on KORALW is 40% lower. The deficit of events is attributed to a

Table 1: Cuts for the acoplanar jet pair selection.

Selection cut	161 GeV	170–172 GeV	181–184 GeV
Visible energy (GeV) <	110	115	115
Transverse acoplanarity (degrees) <	–	–	170
Acollinearity (degrees) >	140	130	120
Modified acoplanarity >	0.1	0.1	0.15
Sphericity <	0.15	Not used	Not used
y_{12} >	Not used	0.4	0.5
Neural Network b tagging >	Not used	1	1.5
OR			
Minimum dijet angle (degrees) <	Not used	40	40
Minimum dijet invariant mass (GeV/c^2) <	Not used	20	20

statistical fluctuation. Since, however, the background is not subtracted in the limit setting, the results are unaffected by systematic uncertainties related to the background estimate.

3.3 Monojet analysis at LEP 1

At energies at and around the Z peak, the topologies associated with the production of an invisible Higgs boson in the reaction $e^+e^- \to hZ^*$ are *(i)* the acoplanar lepton pair, *(ii)* the acoplanar jet pair, and *(iii)* the monojet topologies.

The search for acoplanar jets, optimized for a standard model Higgs boson, produced in the reaction $e^+e^- \to H\nu\bar{\nu}$ and decaying into hadrons, is described in Ref. [4] and was performed using the whole LEP 1 data sample. No candidate events were found, with 1.4 background events expected. The results can be reinterpreted in the present context, with the rôles of the Higgs and Z bosons interchanged.

The search for invisible decay modes of the Higgs boson reported in Ref. [3] was performed using data collected from 1989 to 1992. This analysis has been reoptimized here for the luminosity collected up to 1995, merging the searches for hadronic and leptonic final states into a single monojet selection as in Ref. [20].

The updated selection is as follows. Events must contain at least two good tracks, and the total neutral hadronic energy must be less than 40% of the total visible energy. For events with exactly two good tracks, the total electric charge is required to be zero. The total missing momentum is required to point more than 25.8° away from the beam axis. To suppress the two-photon processes, the total transverse momentum must be greater than $6\%\sqrt{s}$ (increased to $8\%\sqrt{s}$ if the missing momentum points into the regions of vertical cracks in the luminosity calorimeters) and no energy must be detected within 12° of the beam direction. The transverse acoplanarity is required to be less than 140° and no energy within a wedge of 30° around the missing momentum direction in the plane transverse to the beam axis must be detected. The energy in the hemisphere opposite to the total momentum direction is required to be less than 2 GeV. To reject the $e^+e^- \to \tau^+\tau^-$ events in which the decay products of one of the tau's are not reconstructed as energy flow

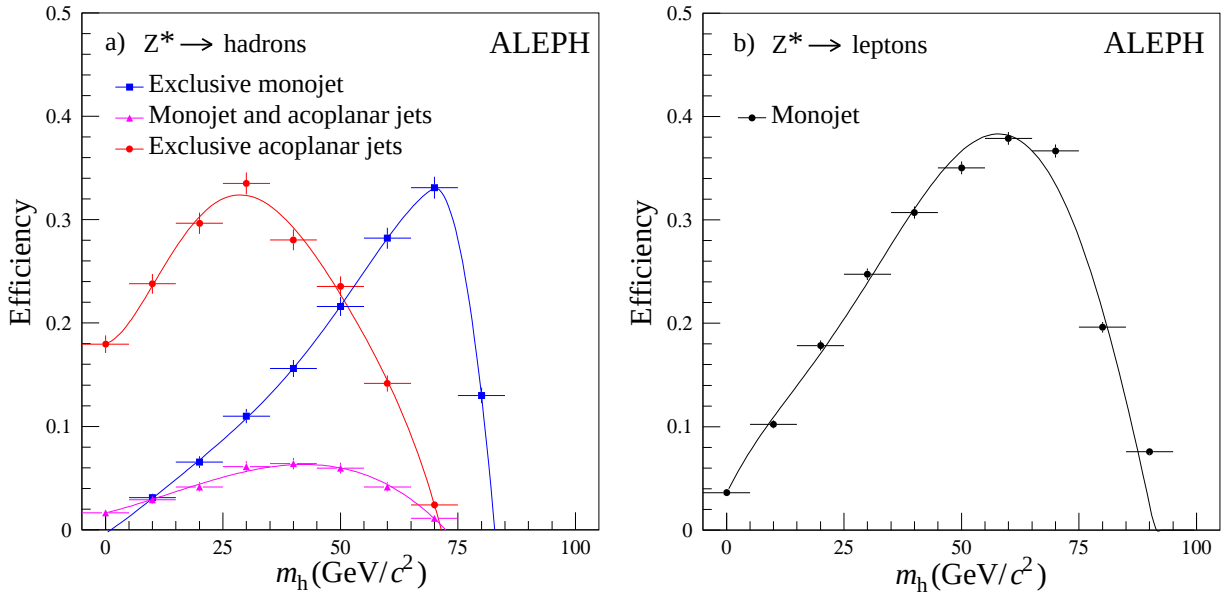

Figure 4: Selection efficiencies as a function of the Higgs boson mass for the LEP 1 analyses. Dots with error bars are the results of the efficiency calculation on Monte Carlo signal samples and the curves represent the parametrization used to set limits. (a) Acoplanar jet selection and monojet selection of the hadronic final states. (b) Monojet selection of the leptonic final states.

objects, evidence for additional tracks in the inner tracking chamber is searched for in events with three and five good tracks. Events in which such an additional track is found in the hemisphere opposite to the total momentum direction are rejected. To remove events with final state radiation, no isolated photon with energy greater than 10 GeV must be detected. Finally, the bulk of the remaining four-fermion background events is eliminated by requiring the visible mass to be greater than 5 GeV/c^2.

The efficiencies of the acoplanar jet and monojet selections for the hadronic final states are shown in Fig. 4a as a function of the Higgs boson mass. The efficiencies are computed for the two samples exclusively selected by either the acoplanar jet or the monojet selection and for the sample selected by both. The efficiency of the monojet selection for the leptonic final states is shown in Fig. 4b. As in the previous section, the systematic uncertainty on the overall efficiency is estimated to be 5%. The requirement that no energy be detected within 12° of the beam axis introduces an inefficiency due to beam-associated background. This loss is monitored with events triggered at random beam crossings and amounts to 5%.

The search for monojet events with the full LEP 1 data sample selected one candidate event, with 2.2 events expected from standard background processes. The missing mass is 69.1 GeV/c^2, with a resolution of 3.1 GeV/c^2. This candidate was already reported in Ref. [20].

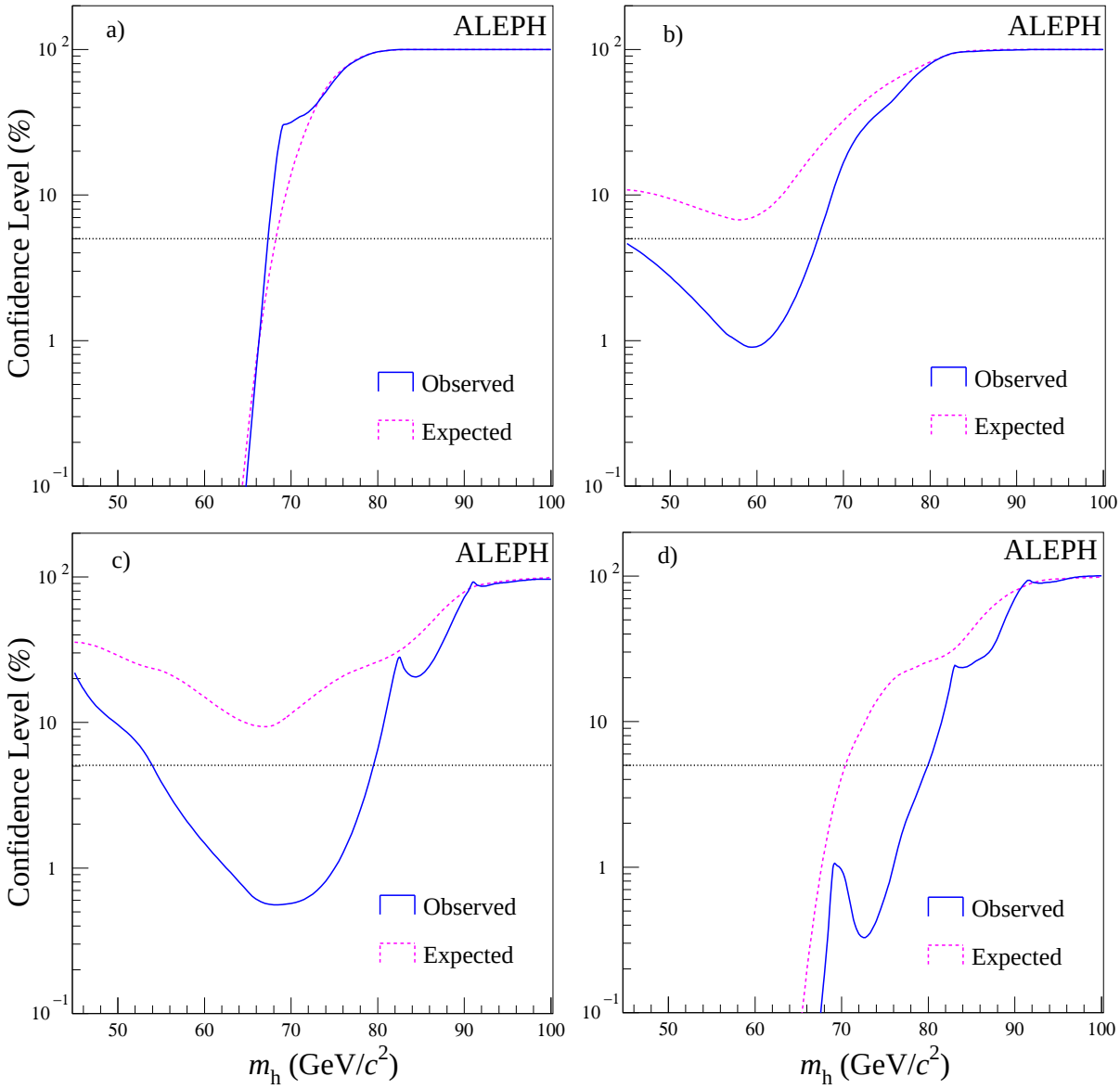

Figure 5: Expected and observed confidence levels as a function of Higgs boson mass, for $\xi^2 = 1$. (a) LEP 1 data; (b) 161 and 170–172 GeV data; (c) 181–184 GeV data and (d) overall combination. The expected confidence levels are based on the PYTHIA generator.

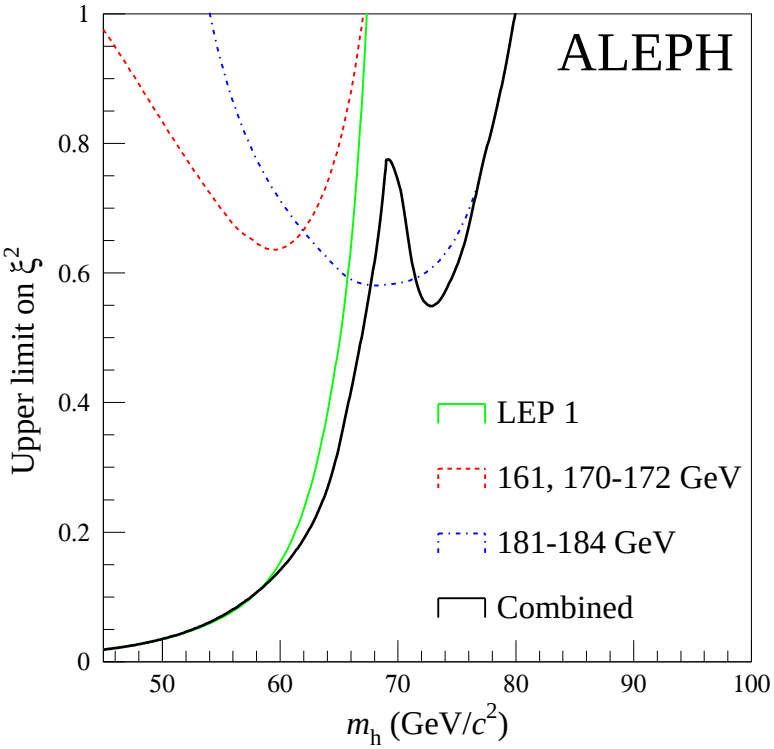

Figure 6: Upper limit on ξ^2 at 95% C.L. as a function of the Higgs mass. The dashed line represents the exclusion region obtained by the analyses with the 161 and 170–172 GeV data sample. The dash-dotted line represents the exclusion region obtained by the analyses with the 181–184 GeV data sample. The grey line is the exclusion region obtained with the full LEP 1 statistics. The black solid line is the exclusion region for the combined results.

4 Combined results

A total of three candidate events was selected in the data by all the searches described in the previous sections (acoplanar lepton pair, acoplanar jet pair and monojet topologies), to be compared with 10 ± 4 events expected from the standard model. The uncertainty in the background estimate comes mainly from the difficult modelling of the energy deposition at the boundaries of the luminosity calorimeters, and from the comparison between different physics generators. The efficiencies, computed with signal Monte Carlo samples, are shown in Fig. 2 and 4 together with the parametrizations used in deriving limits. The calculation of the confidence levels uses the reconstructed Higgs boson mass as a discriminating variable. The systematic uncertainties are taken into account in the derivation of the results according to Ref. [21].

The expected and observed confidence levels as obtained for the combination of the three statistically independent LEP 1 analyses are shown in Fig. 5a as a function of the Higgs boson mass for $\xi^2 = 1$. The results of the search for the Higgs boson in invisible decay modes at 161 and 170–172, and 181–184 GeV are shown in Figs. 5b and 5c, respectively. They are combined in Fig. 5d with those obtained with the LEP 1 data.

The negative results of this search can be translated into 95% C.L. exclusion regions in the (ξ^2, m_h) plane (Fig. 6). As a result, a mass m_h below 80 GeV/c^2 is excluded at

95% C.L. for $\xi^2 = 1$. The average limit expected in the absence of signal is 70 GeV/c^2. With this expected limit, the probability to obtain a limit of at least 80 GeV/c^2 is 16% using the prediction of PYTHIA for the four-fermion background, and 47% using the prediction of KORALW.

5 Conclusions

A search has been made for invisible decay modes of the Higgs boson produced in the reaction $e^+e^- \to hZ$. Acoplanar jet and acoplanar lepton topologies have been studied at centre-of-mass energies of 161, 170–172 and 181–184 GeV. The existing LEP 1 searches for acoplanar jets and monojets, updated to include the full statistics, have been used to derive combined exclusion regions. For a production cross section equal to that of the standard model Higgs boson, a mass m_h less than 80 GeV/c^2 is excluded at 95% C.L.

Acknowledgements

We wish to thank our colleagues from the accelerator divisions for the successful operation of LEP at high energy. We are indebted to the engineers and technicians in all our institutions for their contribution to the excellent performance of ALEPH. Those of us from nonmember countries thank CERN for its hospitality.

References

[1] For a review, see: M. Carena and P.M. Zerwas (Conveners) *et al.* in "Higgs physics at LEP2", Ed: G. Altarelli, T. Sjöstrand, and F. Zwirner, CERN-96-01 (1996) 351.

[2] A. Djouadi, P. Janot, J. Kalinowski, and P.M. Zerwas, *Phys. Lett.* **B376** (1996) 220.

[3] ALEPH Collaboration, "Search for a non-minimal Higgs boson produced in the reaction $e^+e^- \to hZ^*$", *Phys. Lett.* **B313** (1993) 312.

[4] ALEPH Collaboration, "Mass limit for the standard model Higgs boson with the full LEP 1 ALEPH data sample", *Phys. Lett.* **B384** (1996) 427.

[5] L3 Collaboration, "Missing mass spectra in hadronic events from e^+e^- collisions at $\sqrt{s}$ = 161-172 GeV and limits on invisible Higgs decays", *Phys. Lett.* **B418** (1998) 389.

[6] ALEPH Collaboration, "ALEPH: a detector for electron-positron annihilation at LEP", *Nucl. Instrum. and Methods* **A294** (1990) 121.

[7] ALEPH Collaboration, "Performance of the ALEPH detector at LEP", *Nucl. Instrum. and Methods* **A360** (1995) 481.

[8] P. Janot, "The HZHA generator", in Physics at LEP 2, Eds. G. Altarelli, T. Sjöstrand and F. Zwirner, CERN 96-01 (1996) 309.

[9] S. Jadach and Z. Was, *Comp. Phys. Commun.* **36** (1985) 191.

[10] H. Anlauf *et al.*, *Comp. Phys. Commun.* **79** (1994) 466.

[11] J.A.M. Vermaseren in Proceedings of the IVth International Workshop on Gamma Gamma Interactions, Eds. G. Cochard, P. Kessler, Springer Verlag, 1980;
ALEPH Collaboration, "An experimental study of $\gamma\gamma \to$ hadrons at LEP", *Phys. Lett.* **B313** (1993) 509.

[12] T. Sjöstrand, "The PYTHIA 5.7 and JETSET 7.4 Manual", LU-TP 95/20; CERN-TH 7112/93 (1993, revised August 1994); *Comp. Phys. Commun.* **82** (1994) 74.

[13] R. Engel, *Z. Phys.* **C66** (1995) 203;
R. Engel and J. Ranft, *Phys. Rev.* **D54** (1996) 4144.

[14] This generator is based on the differential cross-section published in
S. Ambrosanio and B. Mele, *Nucl. Phys.* **B374** (1992) 3.

[15] M. Skrzypek, S. Jadach, W. Placzek, and Z. Was, *Comp. Phys. Commun.* **94** (1996) 216.

[16] P. Janot and F. Le Diberder, "Optimally combined confidence limits", *Nucl. Instrum. and Methods* **A411** (1998) 449.

[17] ALEPH Collaboration, "Searches for New Particles in Z Decays Using the ALEPH Detector", *Phys. Rep.* **216** (1992) 253.

[18] ALEPH Collaboration, "Search for the standard model Higgs boson in e^+e^- collisions at $\sqrt{s} = 161$, 170 and 172 GeV", *Phys. Lett.* **B412** (1997) 155.

[19] ALEPH Collaboration, "Search for the neutral Higgs bosons of the MSSM in e^+e^- collisions at $\sqrt{s}$ from 130 to 172 GeV", *Phys. Lett.* **B412** (1997) 173.

[20] ALEPH Collaboration, "Observation of monojet events and tentative interpratation", *Phys. Lett.* **B334** (1994) 244.

[21] R.D. Cousins and W.L. Highland, *Nucl. Instrum. and Methods* **A320** (1992) 331.